Structural Significance of the Plasma Membrane Calcium Pump Oligomerization

Valeria Levi, Juan P. F. C. Rossi, Pablo R. Castello, and F. Luis González Flecha
Departamento de Química Biológica, Instituto de Quimica y Fisicoquimica Biologicas, Facultad de Farmacia y Bioquímica, Universidad de Buenos Aires, 1113 Buenos Aires, Argentina

ABSTRACT The oligomerization of the plasma membrane calcium pump (PMCA) in phospholipid/detergent micelles was evaluated using a combined spectroscopic and kinetic approach and related to the enzyme stability. Energy transfer between fluorescein-5′-isothiocyanate and eosin-5′-isothiocyanate attached to different PMCA molecules was used to determine the dissociation constant of dimeric PMCA (140 ± 50 nM at 25°C) and characterize the time course of dimerization. The enzyme thermal stability at different dimer/monomer ratios was evaluated, quantifying the kinetic coefficient of thermal inactivation. This coefficient decreases with PMCA concentration, becoming approximately constant beyond 300 nM. Thermal treatment leads to the formation of inactive monomers that associate only with native monomers. These mixed dimers are formed with a kinetic coefficient that is half that determined for the native dimers. We proposed a model for PMCA thermal inactivation that considers the equilibria among dimers, monomers, and mixed dimers, and the inactivation of the last two species through irreversible steps. The numerical resolution of the differential equations describing this model fitted to the experimental data allowed the determination of the model coefficients. This analysis shows that thermal inactivation occurs through the denaturation of the monomer, which lifetime is 25 min at 44°C. The obtained results suggest that PMCA dimerization constitutes a mechanism of self protection against spontaneous denaturation.

INTRODUCTION

The plasma membrane Ca^{2+} pump is a single-chain integral membrane protein that actively transports Ca^{2+} to the external milieu at the expense of ATP hydrolysis. The aminoacidic chain spans the membrane 10 times, defining short external loops and a large cytoplasmic region (Møller et al., 1996).

The first evidence suggesting that the pump could exist as dimers comes from radiation inactivation experiments on human red cell ghosts (Minocherhomjee et al., 1983; Cavieres, 1984). This study showed that the estimated target size of the plasma membrane calcium pump is 251 kDa, close to twice the size of the monomeric human erythrocyte enzyme. After this initial work, several experimental approaches were used to demonstrate that reversible self-association also occurs if the enzyme is purified and reconstituted in mixed micelles of phospholipids and detergent (Kosk-Kosicka and Bzdega, 1988, 1990; Kosk-Kosicka et al., 1989, 1995; Coelho-Sampaio et al., 1991). It was demonstrated that the pressure-induced dissociation of the Ca^{2+} pump solubilized in micelles of phospholipid and detergent is consistent with a dimer/monomer model (Coelho-Sampaio et al., 1991). Independently, Sackett and Kosk-Kosicka (1996) determined by equilibrium sedimentation the molecular mass of the micelle-solubilized oligomer, reporting a value of 260 kDa.

In a previous article (Levi et al., 2000a), we demonstrated that two different regions are involved in the self-association of the plasma membrane calcium pump (PMCA). One of these regions is highly susceptible to thermal unfolding and was identified as the calmodulin-binding domain. The other region, whose thermal stability is higher than those of the catalytic and calmodulin-binding domains, could be related with the C28W-binding sites.

For many years, it was accepted that the PMCA was activated by self-association (Kosk-Kosicka and Bzdega, 1988). However, recent findings of Bredeston and Rega (1999) cast doubt on this causal relation. In a similar way, other representative members of the P-ATPase family, such as the sarcoplasmic reticulum Ca^{2+} pump (Andersen, 1989) and the Na^+/K^+ pump (Blanco et al., 1994), self associate. It was observed that the monomer of the sarcoplasmic reticulum Ca^{2+}-ATPase and the $\alpha\beta$ protomer of the Na^+/K^+-ATPase are capable of performing all the steps of the reaction cycle (Andersen, 1989; Vilsen et al., 1987). Hitherto, no biological effects associated with the oligomeric forms of these proteins have been found. Because oligomerization is a common feature of this family of proteins, we decided to investigate its significance.

Received for publication 19 April 2001 and in final form 28 September 2001.

Address reprint requests to F. Luis González Flecha, Departamento de Química Biológica-IQUIFIB, Facultad de Farmacia y Bioquímica, Universidad de Buenos Aires, Junín 956, 1113 Buenos Aires, Argentina. Tel.: +54-11-4964-8289; Fax: +54-11-4962-5457;. E-mail lgf@qb.ffyb.uba.ar.

0006-3495/02/01/437/10 $2.00

MATERIALS AND METHODS

Materials

All the chemicals used in this work were of analytical grade and mostly purchased from Sigma Chemical Co. (St. Louis, MO). Eosin-5′-isothiocyanate (EITC) was obtained from Molecular Probes (Eugene, OR). Recently drawn human blood was obtained from the Hematology Section of

the Hospital de Clínicas General José de San Martín (Buenos Aires, Argentina). pH and free Ca^{2+} concentration of the solutions were measured with a Corning pH/ion meter 450, using Orion ion-selective H^+ and Ca^{2+} electrodes (Beverly, MA).

Isolation of membranes from human erythrocytes

Red cells were washed three times with 10 volumes of 150 mM NaCl at 10°C. Calmodulin-depleted erythrocyte membranes were prepared according to González Flecha et al. (1993) using 15 mM MOPS, 1 mM EGTA, and 0.1 mM PMSF (pH 7.4 at 4°C) as hypotonic solution. The membrane suspension was stored at −80°C until PMCA purification.

Purification of Ca^{2+} pump from human erythrocytes

Ca^{2+} pump was isolated in pure form by affinity chromatography. Briefly, calmodulin-depleted erythrocyte membranes were suspended up to 6–8 mg/ml in a buffer composed of 300 mM KCl, 1 mM $MgCl_2$, 100 μM $CaCl_2$, 2 mM DTT, 9.6 mM polyoxyethylene 10 lauryl ether ($C_{12}E_{10}$), 10 mM MOPS (pH 7.4 at 4°C), incubated 10 min at 4°C and centrifuged at 20,000 × *g* for 30 min. The upper phase was supplemented with $C_{12}E_{10}$-solubilized soybean phospholipids up to 0.76 mM and applied to a calmodulin-agarose column. The column was washed with 20-bed volumes of 300 mM KCl, 1 mM $MgCl_2$, 100 μM $CaCl_2$, 800 μM $C_{12}E_{10}$, 290 μM soybean phospholipids, 2 mM DTT, 10 mM MOPS (pH 7.4 at 4°C). This process assures the removal of both membrane proteins different from the PMCA and exchangeable lipids that interact with the pump when it is inserted in the erythrocyte membrane.

Finally, PMCA was eluted in a buffer containing 300 mM KCl, 10 mM MOPS, 1 mM $MgCl_2$, 2 mM EDTA, 2 mM DTT, 800 μM $C_{12}E_{10}$, and 290 μM soybean phospholipids (pH 7.4 at 4°C). After elution, 2 mM $CaCl_2$ was added, giving a free Ca^{2+} concentration of 70 μM. Fractions exhibiting the highest specific Ca^{2+}-ATPase activity were pooled. Integrity of purified Ca^{2+} pump was verified by SDS-PAGE (single band at M_r 134,000) as described previously (Castello et al., 1994). Ca^{2+} pump total mass was determined by densitometric analysis after SDS-PAGE using bovine seroalbumin as standard (P. R. Castello et al., personal communication). The molar concentration of PMCA is expressed as monomeric enzyme. Phospholipid concentration was determined according to Chen et al. (1956). Before use, the enzyme (580 nM, specific ATPase activity 11.5 μmol Pi/mg min) was kept under liquid nitrogen.

Measurement of the Ca^{2+}-ATPase activity

Ca^{2+}-ATPase activity was measured at 37°C as the initial velocity of release of Pi from ATP as described previously (González Flecha et al., 1993), with some modifications. The incubation medium was 7 nM PMCA, 120 mM KCl, 30 mM MOPS, 3.75 mM $MgCl_2$, 1 mM EGTA, 1.1 mM $CaCl_2$, 140 μM soybean phospholipids, 800 μM $C_{12}E_{10}$, and 2 mM ATP (pH 7.4 and $[Ca^{2+}] = 140$ μM). Release of Pi was estimated according to the procedure of Fiske and Subbarow (1925).

Thermal inactivation of the calcium pump

Thermal inactivation experiments were performed by incubating 50 pmol of the Ca^{2+} pump in the reconstitution buffer (elution buffer supplemented with $CaCl_2$ up to $[Ca^{2+}] = 70$ μM). To prevent proteolysis and bacterial growth, it was added to the medium: 3 mM sodium azide, 1 μM pepstatin, 10 μM leupeptin, 1 μg/ml aprotinin, and 0.1 mM PMSF. The tubes were sealed and covered to avoid evaporation and to protect the system from light, and incubated at 25°C until the system equilibrium was reached. The inactivation experiments were run at 44°C, because this process takes place through a common mechanism in the range 33–45°C, and 44°C is the best temperature to accurately evaluate the thermal stability of the calcium pump (Levi et al., 2000b). As was established in that article, the enzyme inactivation is a consequence of its denaturation.

The time course of thermal inactivation is described by the equation,

$$\frac{v}{v_0} = e^{-k_{inact} \cdot t}, \quad (1)$$

where v and v_o are the remaining and the initial activities, t is the incubation time, and k_{inact} is the kinetic coefficient for the thermal inactivation. Because the stability of a protein is inversely related to the rate of its unfolding (Schmid, 1992), we used the kinetic coefficient of thermal inactivation as a measure of the enzyme stability. Thermal-inactivated Ca^{2+} pump was obtained by incubating the enzyme during 7 h at 44°C. After this treatment, the enzyme did not present Ca^{2+}-ATPase activity.

Labeling with fluorescent probes

Ca^{2+} pump was labeled with either fluorescein-5′-isothiocyanate (FITC) or EITC as described previously (Levi et al., 2000a). Calmodulin-depleted erythrocyte membranes were suspended up to 4 mg/ml of protein in a buffer composed of 5 μM $CaCl_2$, 15 mM MOPS, 0.1 mM PMSF (pH = 8.4 at 25°C), and 18 μM of either FITC or EITC. These mixtures were continuously stirred at room temperature in the dark during 30 min for FITC and 60 min for EITC. The reaction was stopped by 10-fold dilution with ice-cold 10 mM Tris-HCl (pH = 8.4). Labeled membranes were washed five times with 5 μM $CaCl_2$, 15 mM MOPS, and 0.1 mM PMSF (pH = 7.4 at 10°C), centrifuging the suspension during 5 min at 20,000 × *g* between washings. After labeling, the Ca^{2+} pump was purified as described above. The complete elimination of the unbound probes was reached during the washing step.

The stoichiometry of labeling was determined by measuring the light absorption in the presence of 1% SDS, 0.1 M NaOH, with the following molar extinction coefficients: 80,000 $M^{-1}cm^{-1}$ at 495 nm for FITC-PMCA and 83,000 $M^{-1}cm^{-1}$ at 522 nm for EITC-PMCA (Munkonge et al., 1988). The extent of labeling with FITC and EITC were 1.1 ± 0.1 and 0.93 ± 0.2 mol of probe per mole of ATPase monomer, respectively.

After labeling with FITC or EITC, the enzyme completely lost its Ca^{2+}-ATPase activity. The inhibition of the enzyme by FITC is a consequence of the selective binding of this probe to lysine 495 in hPMCA4b isoform residue located near the ATP binding site (Filoteo et al., 1987). In the labeling conditions used in this work, EITC and FITC bind to the same site (Gatto and Milanick, 1993). These authors observed that the enzyme is not able to bind ATP after chemical modification with either of these probes. In addition, the enzyme properties that do not depend on ATP binding are conserved after the specific labeling. Particularly, the labeled enzymes preserve the ability to bind calmodulin in a Ca^{2+}-dependent mode, exhibit calmodulin-dependent phosphatase activity (Donnet et al., 1998), and dimerize (Levi et al., 2000a). The thermal stabilities of the derivatized enzymes and the nonlabeled enzyme are not significantly different (Levi et al., 2000a). These results suggest that FITC and EITC introduce minor structural modifications in the protein and thus, they probe the native conformation of the Ca^{2+} pump.

Spectroscopic measurements

Absorption measurements were performed in a Shimadzu UV-160 A spectrophotometer using a 1-cm pathlength cuvette. Fluorescence emission spectra were recorded in a 3 × 3 mm quartz cuvette using a SLM-AMINCO BOWMAN Series 2 spectrofluorometer (Spectronic Instrument Inc., Rochester, NY). The temperature was set at 25°C except where it is indicated. The excitation wavelength was 495 nm (FITC-PMCA) and 295 nm (PMCA), and the excitation and emission bandwidths were set at 4 nm.

Appropriate blanks corresponding to the reconstitution buffer were subtracted from the measurements to correct background fluorescence.

The wavenumber corresponding to the center of spectral mass of the Ca^{2+} pump ($\bar{\nu}_{CM}$) was determined according to Silva et al. (1986),

$$\bar{\nu}_{CM} = \frac{\int I_{PMCA(\bar{\nu})}\bar{\nu}\, d\bar{\nu}}{\int I_{PMCA(\bar{\nu})}\, d\bar{\nu}} \cong \frac{\sum_i I_{PMCA(\bar{\nu}_i)}\bar{\nu}_i\Delta\bar{\nu}_i}{\sum_i I_{PMCA(\bar{\nu}_i)}\Delta\bar{\nu}_i}, \quad (2)$$

where $I_{PMCA(\bar{\nu}_I)}$ stands for the fluorescence emitted at wavenumber $\bar{\nu}_i$. The emission spectra of the system composed of FITC-PMCA (donor) and EITC-PMCA (acceptor) is a linear combination of the emission spectra of each species as

$$I(\lambda) = \sum_j \omega_j \cdot I_j^o(\lambda), \quad (3)$$

where $I(\lambda)$ is the emission intensity of the mixture, $I_j^o(\lambda)$ is the emission intensity spectrum of the isolated j component, and ω_j is the weight factor of each component in the spectrum of the mixture.

Deconvolution of the spectra in the individual FITC-PMCA and EITC-PMCA spectra was done by fitting Eq. 3. The FITC-PMCA fluorescence intensity in a given mixture was calculated according to

$$I_{FITC\text{-}PMCA} = \omega_{FITC\text{-}PMCA} \sum_i I^o_{FITC\text{-}PMCA}(\lambda_i) \cdot \Delta\lambda_i. \quad (4)$$

The apparent efficiency of fluorescence energy transfer (E_{app}) was measured from the decrease on the donor fluorescence caused by the presence of the acceptor according to the equation

$$E_{app} = 1 - \frac{I_{FITC\text{-}PMCA}}{I^o_{FITC\text{-}PMCA}}, \quad (5)$$

where $I_{FITC\text{-}PMCA}$ and $I^o_{FITC\text{-}PMCA}$ are the FITC-PMCA emission intensity in the presence or the absence of EITC-PMCA, respectively.

Determination of the PMCA dissociation constant

E_{app} can be related to the concentration of the heterodimer formed by FITC-PMCA and EITC-PMCA molecules (DA), in a similar way as was proposed for gramicidin dimerization by Veatch and Stryer (1977),

$$E_{app} = E\frac{[DA]}{[D]_T}, \quad (6)$$

where $[D]_T$ is the total donor concentration, and E represents the maximal efficiency of the energy transfer process if the only Ca^{2+} pump species in the system were the heterodimer. This equation considers that the fluorescence of the donor is not affected by association with other donor molecule. When the donor–acceptor mole ratio is 1, the following relation is obtained:

$$E_{app} = \frac{E}{2}\left[1 + \frac{1}{8[D]_T}\left(K_{dis} - (K_{dis}^2 + 16K_{dis}[D]_T)^{1/2}\right)\right], \quad (7)$$

where K_{dis} is the dissociation constant of the Ca^{2+} pump dimer.

Data analysis

All measurements were performed in duplicate or triplicate. The equations were fitted to the experimental data using a nonlinear regression procedure based on the Gauss–Newton algorithm (Seber and Wild, 1989). The dependent variable was assumed to be homoscedastic (constant variance), and the independent variable was considered to have negligible error. Parameters were expressed as the mean ± SE.

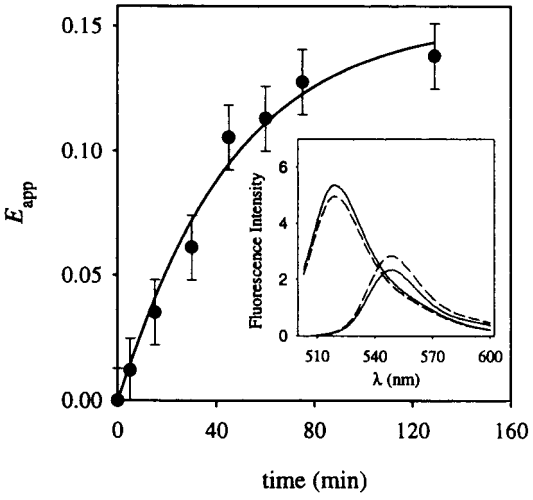

FIGURE 1 Time course of energy transfer between FITC-PMCA and EITC-PMCA. Purified FITC-PMCA was supplemented with EITC-PMCA up to equimolar condition (total Ca^{2+} pump concentration, 480 nM) and the emission spectrum of the mixture was recorded at different times. The apparent efficiency of energy transfer was calculated from these data as described in Materials and Methods and plotted as a function of time. Solid line represents the time series of E_{app} constructed using the final set of parameter values obtained for the exchange reactions shown in Scheme 8 (see the text for details). *Inset*: emission spectra of FITC-PMCA and EITC-PMCA (*solid line*). The dotted lines correspond to the spectra obtained by deconvolution of the spectrum measured after mixing for 1.5 h FITC-PMCA and EITC-PMCA up to the concentrations previously mentioned. The spectra centered at 520 and 560 nm correspond to FITC and EITC emissions, respectively.

RESULTS

Quantitative description of the oligomerization equilibrium of the Ca^{2+}pump

Fluorescence resonance energy transfer from FITC-PMCA to EITC-PMCA was used to monitor the dimerization process of the solubilized Ca^{2+} pump. This procedure was successfully applied to study self association in many proteins, for example, the Ca^{2+} pump of erythrocyte membranes (Levi et al., 2000b) and of sarcoplasmic reticulum (Papp et al., 1987). Figure 1 shows the fluorescence spectra of both isolated species (*solid lines* in the inset), and those obtained by deconvolution of the spectrum measured after mixing the donor- and the acceptor-labeled pumps (*dashed lines*). The decrease of the fluorescence intensity corresponding to the FITC peak concomitantly with the increase of the intensity of the EITC peak reflects the energy transfer between the probes and, thus, the association between the labeled enzymes.

The time course of the apparent efficiency of energy transfer (E_{app}) is shown in Fig. 1. Initially, the dimers

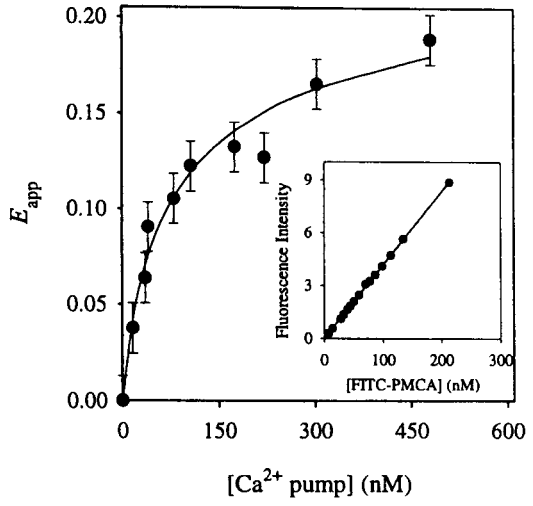

FIGURE 2 Dependence of the apparent efficiency of energy transfer on protein concentration. Purified FITC-PMCA was supplemented with EITC-PMCA up to equimolar condition (total Ca^{2+} pump concentration 480 nM) and mixed for 1.5 h. Total enzyme concentration of this sample and of a control without EITC-PMCA was modified by serial dilution, while the concentration of other components were held constant. The emission spectrum after each dilution step was recorded after the steady state was reached. The apparent efficiency of energy transfer was plotted as a function of the total protein concentration. Solid line is the graphical representation of Eq. 7 with the best-fitting parameter values indicated in the text. *Inset*: Fluorescein emission intensity of the control without EITC-PMCA was plotted as a function of FITC-PMCA concentration.

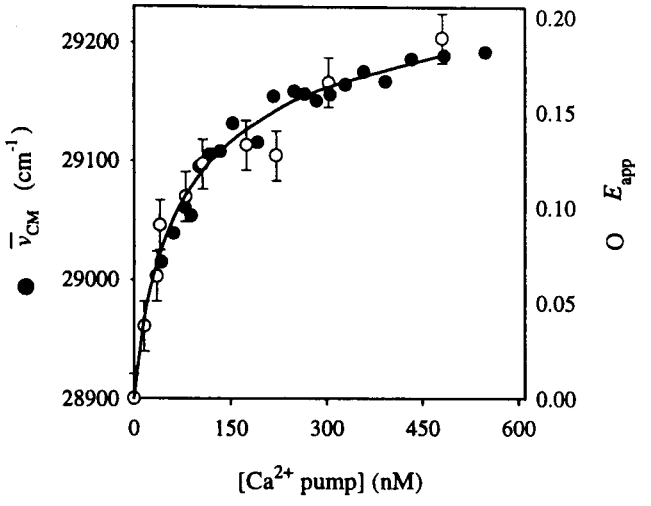

FIGURE 3 Changes on the PMCA fluorescence spectrum produced by enzyme dilution. Purified Ca^{2+} pump was diluted with the reconstitution buffer up to different protein concentration in the range 30–360 nM. The emission spectrum after each dilution was recorded after the steady state was reached. The center of spectral mass was calculated as described in Materials and Methods and plotted as a function of the total protein concentration (●). Values of apparent efficiency of energy transfer were taken from Fig. 2 (○). Solid line represents the fitting of Eq. 7 to the energy transfer data.

present in the system are composed of two FITC-PMCA or two EITC-PMCA molecules. When the species are mixed, the exchange between dimer subunits is produced, leading to the formation of the heterodimer with a consequent increase on E_{app}.

The dissociation equilibrium of Ca^{2+} pump was analyzed by measuring the dependence of E_{app} on the total enzyme concentration. Figure 2 shows that energy transfer increases with the enzyme concentration, becoming approximately constant beyond 300 nM. FITC-PMCA fluorescence in the absence of the acceptor was measured as a control and found to be linearly related to its concentration, indicating that the emission intensity of FITC is not affected by the association between FITC-PMCA molecules (Fig. 2, *inset*). Eq. 7 was fitted to the experimental data, obtaining $K_{dis} = 140 \pm 50$ nM and $E = 0.53 \pm 0.07$.

As a control, we determined the centers of mass of the emission spectra of the unlabeled Ca^{2+} pump at different enzyme concentrations. Figure 3 shows a blue shift of 200 cm^{-1} in the fluorescence spectrum with increasing Ca^{2+} pump concentration until 300 nM, where the position of the spectrum became approximately constant. It can be observed that the dependence of the center of spectral mass on the enzyme concentration is similar to that verified for the apparent efficiency of energy transfer. The energy transfer between FITC-PMCA and EITC-PMCA monitors the subunit interchange reactions resulting from the equilibria,

$$A_2 \underset{k_2}{\overset{k_1}{\rightleftharpoons}} A + A \quad D_2 \underset{k_2}{\overset{k_1}{\rightleftharpoons}} D + D \quad DA \underset{k_2}{\overset{k_1}{\rightleftharpoons}} D + A \qquad (8)$$

where D and A represents the donor and acceptor molecules, k_1 and k_2 are the kinetic coefficient of dimer dissociation and monomers association, respectively. The differential equations describing these reactions were fitted to the data shown in Fig. 1 using the procedure described in the Appendix with the following boundary conditions: $k_1/k_2 = K_{dis} = 140$ nM, $E = 0.53$ and $[DA]_o = 0$. The final values for the kinetic coefficients were $k_1 = 1.24 \pm 0.50\ h^{-1}$ and $k_2 = 8.8 \times 10^{-3} \pm 2.4 \times 10^{-3}\ nM^{-1}h^{-1}$.

Effects of oligomerization on the calcium pump thermal stability

Figure 4 shows the dimer and monomer distribution along the protein concentration range assayed in the experiments shown in Figs. 2 and 3. This information was used to select specific values of enzyme concentration to evaluate the dimerization effects on PMCA thermal stability within a wide range of dimer/monomer ratios. The time course of the calcium pump thermal inactivation at 44°C was evaluated after dilution of the nonlabeled enzyme up to different PMCA concentrations (Fig. 5 *A*). Because the enzyme di-

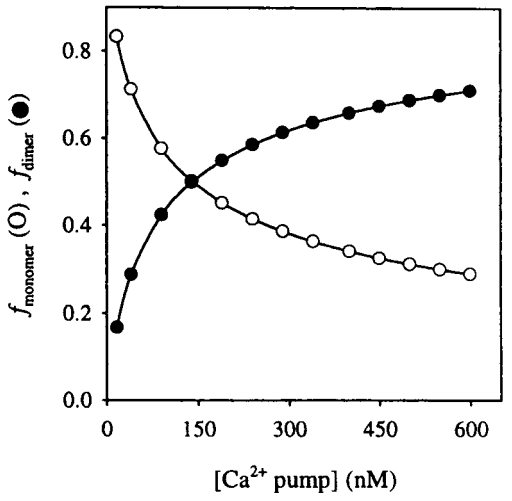

FIGURE 4 Ca^{2+} pump dimer and monomer distribution. The fractions of the enzyme as dimer (●) and monomer (○) were calculated for different total Ca^{2+} pump concentration in the range 15–580 nM using K_{dis} = 140 nM.

lution was performed with the reconstitution buffer, the PMCA concentration is the only modification on the system composition. The kinetic coefficients obtained by fitting Eq. 1 to these experimental data are represented as a function of the PMCA concentration (Fig. 5 *B*). It can be observed that the enzyme thermal stability increases with the protein concentration, with a higher dependence at low concentrations.

Mixed dimers formation and stability

In a previous article (Levi et al., 2000a), we demonstrated that energy transfer between FITC-PMCA and EITC-PMCA is completely lost after thermal denaturation of both labeled enzymes. This evidence indicates that the inactive enzyme is unable to self associate. Conversely, thermal denaturation of only the acceptor did not affect the energy-transfer efficiency. Thus, we can conclude that thermal-inactivated enzyme can associate with an active molecule, forming a mixed dimer.

The kinetics of mixed dimer formation was evaluated following the procedure described in Fig. 1 after preincubating EITC-PMCA 7 h at 44°C (data not shown). Kinetic coefficients of subunits association and mixed dimer dissociation were determined fitting the differential equations characterizing the reactions shown in Scheme 8, as was previously described. Because the thermally inactivated PMCA is not able to self associate, the equilibrium involving only EITC-PMCA species was not considered for the fitting. The final values for the kinetic coefficients were $1.07 \pm 0.50\ h^{-1}$ (mixed dimer dissociation) and $3.9 \times 10^{-3} \pm 1.0 \times 10^{-3}\ nM^{-1}h^{-1}$ (association between native and thermal denatured monomers).

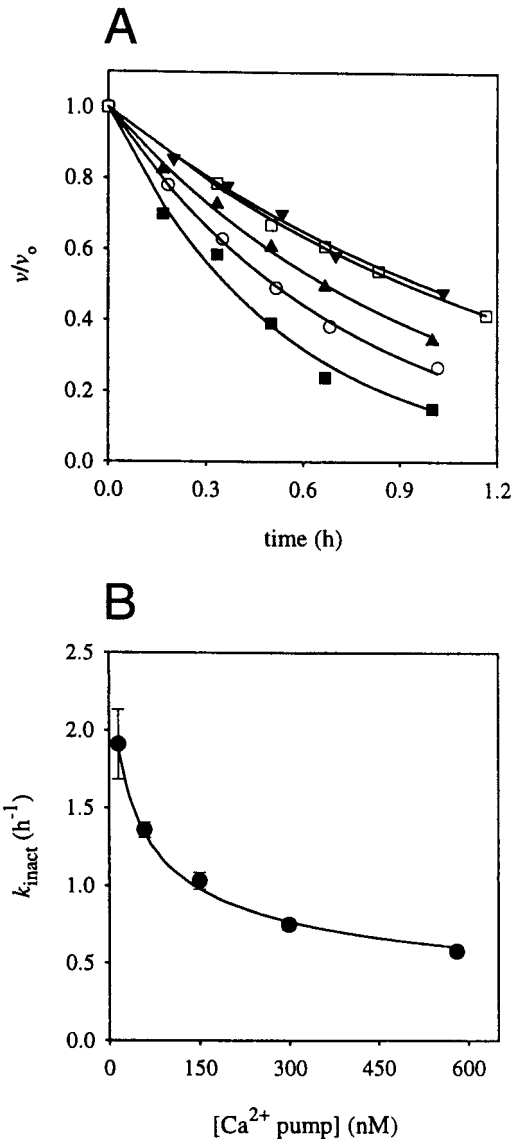

FIGURE 5 Dependence of thermal inactivation kinetics on the Ca^{2+} pump concentration. (*A*) Purified Ca^{2+} pump concentration was adjusted at (nM): 580 (▼), 300 (□), 150 (▲), 58 (O) and 15 (■), keeping constant the concentration of the other components of the medium. The specific enzyme activity was measured after the equilibration and was found to be independent of the Ca^{2+} pump concentration within the assayed range. Thermal inactivation was performed at 44°C as described in Materials and Methods. At different times, aliquots were taken, Ca^{2+}-ATPase activity was measured and expressed relative to the initial activity. Solid lines are the graphical representation of Eq. 1 fitted to the experimental data. (*B*) The values of the kinetic coefficients for thermal inactivation were plotted as a function of protein concentration. Solid line represents the values of k_{inact} predicted for the inactivation model (Scheme 9). These values were obtained by fitting Eq. 1 to the time series of v/v_o constructed using the final values of the model parameter (see Appendix for details).

To study the thermal stability of the native enzyme when it is forming mixed dimers, we assayed the kinetics of the PMCA thermal inactivation in a mixture composed of 40 nM native enzyme and 520 nM thermal-inactivated enzyme

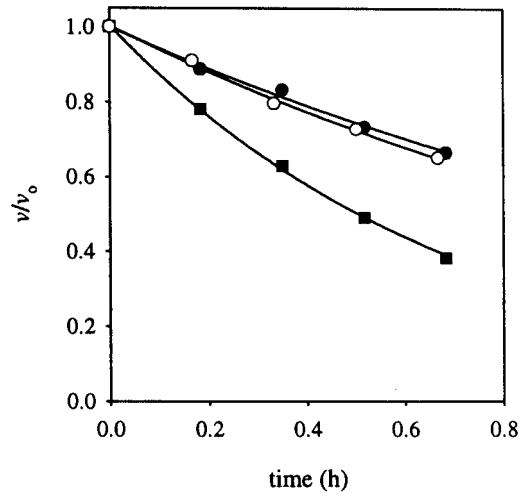

FIGURE 6 Time course of mixed dimer thermal inactivation. Native and thermal-inactivated Ca^{2+} pump were mixed up to 40 and 520 nM, respectively. This preparation (O) and two fractions containing either 560 nM (●) or 40 nM (■) of native enzyme were incubated at 44°C as described in Materials and Methods. Aliquots were taken at different times, Ca^{2+}-ATPase activity was measured and expressed relative to the initial activity. Solid lines are the graphical representations of Eq. 1 fitted to the experimental data. The kinetic coefficients were: 0.59 ± 0.05 h^{-1} (40 nM native enzyme + 520 nM denatured enzyme), 1.36 ± 0.04 h^{-1} (40 nM native enzyme) and 0.64 ± 0.05 h^{-1} (560 nM native enzyme).

(Fig. 6). The inactivation coefficient determined in this condition was similar to that measured for the same total enzyme concentration (560 nM), being significantly lower than the value obtained for the same native enzyme concentration (40 nM).

DISCUSSION

Throughout this work, we explored the relevance of PMCA dimerization to the enzyme stability. Because the stability of the protein is related with its three-dimensional structure, this study provides information about the structural changes that take place during dimerization.

Dimerization equilibrium of the PMCA

Ca^{2+} pump dissociation equilibrium was analyzed by two different procedures. We measured the dependence of the apparent efficiency of energy transfer between FITC-PMCA and EITC-PMCA on the protein concentration (Fig. 2) and determined the value of K_{dis}. This value is near the range previously estimated by Coelho-Sampaio et al. (1991) despite some differences in the medium composition.

Additionally, we verified that dilution of the nonlabeled enzyme promoted a red shift of the fluorescence spectrum (Fig. 3), similar to that observed by Coelho-Sampaio et al. (1991). This behavior has been reported to occur on dissociation of several oligomeric proteins as a consequence of the exposure of tryptophan residues previously buried in the intersubunit's interface to the aqueous medium (Weber, 1987).

We verified a similar dependence of E_{app} and $\bar{v}_{CM}$ with the enzyme concentration suggesting that the labeling of the enzyme with FITC and EITC did not affect the association between subunits. Thus, the dissociation constant determined by energy transfer can be assigned to the unlabeled PMCA.

Fitting Eq. 7 to data shown in Fig. 2 also provided the value of the FRET efficiency for the dimer molecule (E). This parameter depends on the photochemical properties of the system and on the distance between FITC and EITC. Considering that R_o for this donor–acceptor pair is 50.3 Å (Levi et al., 2000a), the average distance between FITC and EITC attached to Ca^{2+} pump molecules forming a heterodimer was 49.3 Å (see Lakowicz, 1983; for details of this calculation). This value is approximately half the width of the cytoplasmic domain of a related P-ATPase, i.e., the sarcoplasmic reticulum Ca^{2+}-ATPase (Toyoshima et al., 2000).

The energy transfer measurements were also used to evaluate the kinetics of native and mixed dimers formation. The kinetic coefficients for the dissociation of both kinds of dimer are not significantly different, agreeing with our previous results, which suggest that the interface between subunits is identical in native and mixed dimers (Levi et al., 2000a). In addition, the kinetic coefficient of mixed dimer formation is approximately half that obtained for the active monomers association. Because one of the dimerization domains of the inactive monomer is denatured (i.e., the calmodulin binding domain), only one of the two forms of association of PMCA monomers that lead to native dimers is possible in the formation of mixed dimers. Thus, the probability of mixed dimer formation should be half that corresponding to the native dimer, in agreement with the experimental result.

Thermal inactivation dependence on PMCA self association

Figure 5 shows that thermal stability of the PMCA decreases after dilution of the enzyme. This experiment, as those shown in Figs. 2 and 3, was performed keeping constant the composition of the medium including phospholipid and detergent, which constitute the mixed micelles where the Ca^{2+} pump is solubilized. In a previous work, we demonstrate that amphipiles modulate the enzyme activity and stability through a motionally restricted monolayer that covers the transmembrane domain of the pump (Levi et al., 2000b). The composition of this monolayer is determined by the micelle composition and the relative affinity of the amphiphiles for the hydrophobic surface of the protein. This affinity was not dependent on the protein concentration (results not shown). Thus, the amphiphiles environment of

the PMCA transmembrane domain is not modified throughout the experiments shown in Figs. 2, 3, and 5. Additionally, we demonstrated that the stability of the enzyme is maximal and slightly dependent on the micelle composition if phospholipid molecules cover more than 80% of the transmembrane surface (Levi et al., 2000b). In the present work, the composition of the micelles was chosen to fulfill this condition. Besides, the exchangeable erythrocyte membrane phospholipids initially adsorbed to the PMCA are removed during the washing step of the enzyme purification procedure. Therefore, they are not involved in the phenomenon observed in Fig. 5. According to these observations, the only modification on the system occurring during the dilution of the enzyme is the increase of the dissociation degree of PMCA. As a consequence, the behavior observed in Fig. 5 suggests a higher stability of the enzyme in its dimeric form.

A model for thermal inactivation of the Ca^{2+} pump

According to the results described above, we propose the following mechanism for the thermal inactivation of the Ca^{2+} pump:

$$\begin{array}{ccccc} & + & M & \underset{k_1}{\overset{k_2}{\rightleftarrows}} & M_2 \\ M & & \downarrow k_3 & & \downarrow k_4 \\ & + & M_i & \underset{k_1}{\overset{1/2k_2}{\rightleftarrows}} & M_iM \end{array} \qquad (9)$$

The native monomer (M) is denatured following an irreversible step that leads to the formation of the inactive monomer (M_i). M can also associate with a native or an inactive monomer to form a native dimer (M_2) or a mixed dimer (M_iM). Furthermore, it is included in the transformation of the native dimer into a mixed dimer through an irreversible step.

Figure 4 shows that, within the experimentally allowed concentration range, the dimeric and monomeric species are in significant amounts in the initial system. Therefore, k_{inact} is a complex combination of the kinetic coefficients of the steps of the thermal inactivation model. These coefficients can be calculated fitting the model to the experimental data from Fig. 5 and using the iterative procedure described in the Appendix. For this task, we considered as initial value of k_3, the k_{inact} obtained at the lowest enzyme concentration shown in Fig. 5 *B* and, for k_1 and k_2, those previously determined from energy transfer experiments at 25°C. The exchange between dimers' subunits at this temperature is not accompanied by thermal denaturation of the enzyme. Because k_4 cannot be estimated experimentally, we performed the fitting, considering initial values of this parameter within a wide range ($0–30\ h^{-1}$).

In addition, that the relative activity is related to the concentration of the active species was taken into account as

$$\frac{v}{v_o} = \frac{\alpha \cdot [M_2] + \beta \cdot [M] + \gamma \cdot [M_iM]}{\alpha \cdot [M_2]_o + \beta \cdot [M]_o}, \qquad (10)$$

where α, β, and γ are the molar activities of the native dimer, the native monomer, and the mixed dimer, respectively. This equation considers that the enzyme is completely active at the initial state. Because the specific enzyme activity is independent of the Ca^{2+} pump concentration within the assayed range, $\alpha = 2\beta$. Additionally, the same specific activities of the heterodimer and the native monomer were assumed. Then, Eq. 10 can be expressed as

$$\frac{v}{v_o} = \frac{2 \cdot [M_2] + [M] + [M_iM]}{2 \cdot [M_2]_o + [M]_o}. \qquad (11)$$

To perform the iterative procedure, we considered the following boundary conditions: a) only M and M_2 are initially present in the system, and b) their initial concentrations are defined by the ratio k_1/k_2.

The final parameter values of the inactivation model were: $k_1 = 4.0 \pm 0.6\ h^{-1}$, $k_2 = 4.2 \times 10^{-2} \pm 1.0 \times 10^{-2}\ nM^{-1}h^{-1}$, $k_3 = 2.43 \pm 0.05\ h^{-1}$ and $k_4 = 0 \pm 0.05\ h^{-1}$. The solid line in Fig. 5 shows that the time series of k_{inact}, constructed from the final set of parameter values corresponding to the inactivation model, agrees with the experimental data.

Analysis of the thermal inactivation model

Figure 7 shows the time course of the different species included in the inactivation model at both extremes of the concentration range assayed in the experiment shown in Fig. 5. It can be observed that formation of native and mixed dimers decreases the rate of inactivation by capturing the native monomer molecules, which can undergo thermal inactivation.

The values obtained for k_1 and k_2 after the convergence of the iterative procedure correspond to the kinetic coefficients for dimer dissociation and monomers association at 44°C. The ratio k_1/k_2 at 44°C was not significantly different from K_{dis} measured at 25°C, indicating a similar distribution of the species at both temperatures.

To test whether the model is in good consistence with experimental data not considered for its construction, we performed the comparative analyses described below. First, we used the final values of the kinetic coefficients to predict the time course of energy transfer between FITC-PMCA and EITC-PMCA at 44°C. For this purpose, we considered that the labeled molecules are denatured according to the inactivation model, and that the native and mixed dimer can be homo- or hetero-labeled species. The time course of the concentration of the species was calculated using the dif-

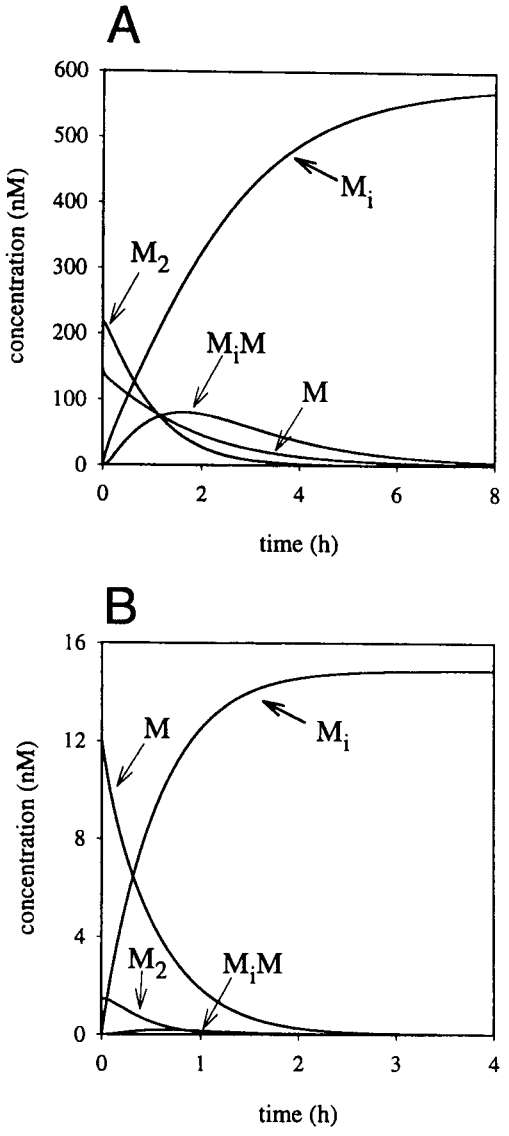

FIGURE 7 Time course of the PMCA species during thermal inactivation at 44°C. Time series of the concentration of the species at total enzyme concentration of (*A*) 580 nM or (*B*) 15 nM were calculated by numerical resolution of the differential equations that describe the inactivation model with the final parameter values indicated in the text.

ferential equations in Schemes 8 and 9, and Eq. A1. E_{app} series could be constructed from these data using Eq. 6 and the parameter E at 44°C. However, this parameter is unknown and could not be evaluated because the enzyme would denature during the time required for its determination. Therefore, we constructed a series relative to the value of E_{app} at a specific time (i.e., 10 min). Figure 8 shows this simulation (*solid line*) and data obtained from an experiment of energy transfer similar to that shown in Fig. 1, but at 44°C. This figure shows that the model prediction agrees with the experimental data. In addition, Fig. 8 also includes a simulation of the time course of energy transfer at 44°C in

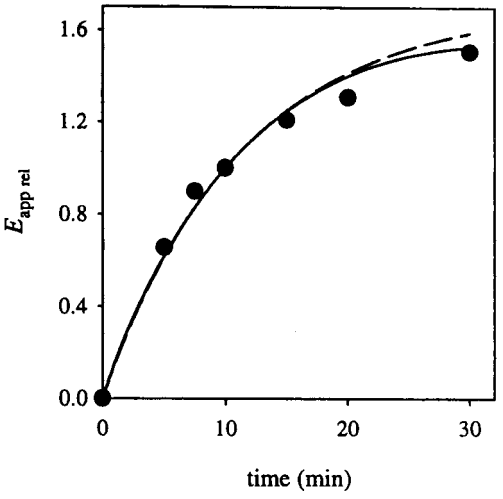

FIGURE 8 Time course of energy transfer between FITC-PMCA and EITC-PMCA at 44°C. Purified FITC-PMCA was supplemented with EITC-PMCA up to equimolar condition (total Ca^{2+} pump concentration, 480 nM). The system was incubated at 44°C and the emission spectrum was recorded at different times. E_{app} was calculated from these data as described in Materials and Methods. The apparent efficiency of energy transfer relative to that measured after 10 min of incubation ($E_{app,rel}$) was plotted as a function of time. Time series for the concentrations of the different species were generated by numerical resolution of the differential equations describing the reactions shown in Schemes 8 and 9, using the final set of parameter values and transformed in $E_{app,rel}$ values (*solid line*). The dashed line represents the time series of $E_{app,rel}$ constructed from the exchange reactions shown in Scheme 8 with $k_1 = 4.95\ h^{-1}$ and $k_2 = 5 \times 10^{-2}\ nM^{-1}h^{-1}$. In both cases, it was considered that the enzyme is completely native at the initial state and $[DA]_o = 0$. $E_{app,rel}$ was calculated from the time series of [DA] using Eq. 6.

which the inactivation of the enzyme was not considered (*dashed line*). The simulated time course agrees with the experimental data during the initial 15 min of incubation, indicating that the enzyme denaturation is negligible within this time period.

To further explore the predictive value of the inactivation model, we compared the simulated inactivation kinetics, in conditions in which the main dimeric form is the mixed dimer, with that experimentally determined (Fig. 6). The initial concentration of each species was calculated using the dissociation constant values of the native and mixed dimer, and considering that the system is initially composed of 520 nM inactive enzyme and 40 nM active enzyme. Time series for species concentrations were numerically calculated using Eq. A1 and transformed into time series of enzyme activity using Eq. 11. This series follows an exponential function with $k_{inact} = 0.56 \pm 0.01\ h^{-1}$, which is not significantly different from the inactivation coefficient experimentally determined ($0.59 \pm 0.05\ h^{-1}$).

Concluding remarks

Results shown in this work indicate that thermal inactivation of the calcium pump occurs through monomer dena-

turation, suggesting that dimerization could constitute a mechanism of self protection against spontaneous inactivation. It is possible that specific PMCA ligands modulate this mechanism. In fact, it is known that Ca^{2+} and calmodulin enhance the calcium pump stability (Pikula et al., 1991; Garrahan and Rega, 1990). However, there is not a single mechanism to explain the effects of these ligands on the enzyme stability and dimerization. For instance, Ca^{2+} enhances both the stability and the dimerization of the enzyme, whereas calmodulin enhances the enzyme stability but dissociate the PMCA dimers. The interpretation of these effects is complex and requires a careful study, currently in progress in our laboratory.

Since PMCA dimerization was described, some efforts were performed to relate it to the functional and biological role of the enzyme. Initially, Sackett and Kosk-Kosicka (1996) proposed that the dimer is the active species of the PMCA in the absence of calmodulin. In contrast, the results of Bredeston and Rega (1999) indicate that the monomer and the dimer have the same specific activity. It was also suggested that transient associations between monomers during cation-pump cycles might be a common feature of the ion-translocation mechanism in P-ATPases (Boldyrev and Quinn, 1994). In this work, we demonstrated that PMCA self association in mixed micelles occurs in the range of minutes. Besides, the enzyme completes the elementary reactions of the cycle—in the presence of ATP, Ca^{2+}, and Mg^{2+}—in the range of milliseconds (Garrahan and Rega, 1990). Thus, it seems unlikely that changes in the oligomerization state of the enzyme occur during the catalytic cycle.

Finally, we have observed that the lifetime of the Ca^{2+} pump in the erythrocyte membrane is 20 ± 4 h at 44°C (V. Levi, et al., unpublished), which is ~10-fold higher than that determined in artificial bilayers (Levi et al., 2000b). Thus, the self-protection mechanism described in this work for the PMCA solubilized in mixed micelles should be extended to PMCA in the erythrocyte membrane, where the enzyme is mainly dimeric.

APPENDIX

Iterative procedure for fitting kinetic-models to time series

After identifying a tentative model for a given process, the next step is to find the set of parameter values that give the best fit to the observed data. A frequently used criterion of best fit is that of least squares, in which the parameter values are selected to minimize the sum of the squares deviations (S) between the observed data (y_i) and the values calculated from the model (f_i). Because the processes studied in this work conduce to a set of nonintegrable differential equations, the least-squares method must be used in combination with the numerical resolution of these equations. For this purpose, we used the simplest numerical method (Euler method) that uses the first derivative to estimate the function a short step Δt away from an initial value,

$$[X]_{j,(t+\Delta t)} = [X]_{j,(t)} + \left(\frac{\Delta[X]}{\Delta t}\right)_t \Delta t. \qquad \text{(A1)}$$

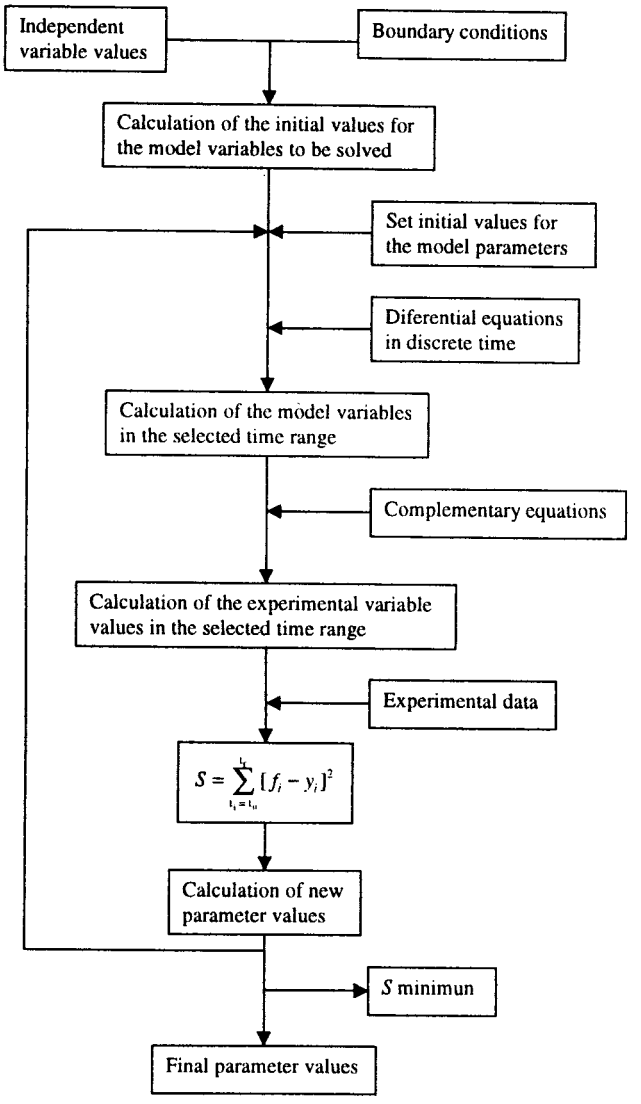

FIGURE A1 Iterative procedure for fitting kinetic-models to time series.

Figure A1 describes the iterative procedure used for these calculations.

In this work, the model variables (X_j) are the concentrations of the species, the independent variable is the total enzyme concentration, and the experimental variables are E_{app} (Fig. 1) or v/v_o (Fig. 5 *A*). The initial values for the model variables were calculated using the particular boundary conditions described in the text for each process and the independent variable values.

Once the initial set of parameter values was chosen, the set of differential equations describing the model was numerically solved allowing the construction of time series of the model variables. These series were used to build time series of the experimental variables (E_{app} and v/v_o), applying the complementary equations (Eqs. 6 and 11 for Schemes 8 and 9, respectively). Using a least-squares method, a new set of parameters was ob-

tained. The regression procedure was used iteratively with the new parameter values as the starting set for a further cycle of refinement. This process was continued until the computed parameter adjustments became negligible. The iteration was then said to have converged, and the set of parameter values corresponded to a minimum of *S*. The standard deviation of the parameters was then calculated from the correlation matrix according to the procedure described by de Levie (1999).

This work was supported by grants from UBACYT and CONICET.

REFERENCES

Andersen, J. P. 1989. Monomer–oligomer equilibrium of sarcoplasmic reticulum Ca-ATPase and the role of subunit interaction in the Ca^{2+} pump mechanism. *Biochim. Biophys. Acta.* 988:47–72.

Blanco, G., J. C. Koster, and R. W. Mercer. 1994. The alpha subunit of the Na, K-ATPase specifically and stably associates into oligomers. *Proc. Natl. Acad. Sci. U.S.A.* 91:8542–8546.

Bredeston, L. M., and A. F. Rega. 1999. Phosphatidylcholine makes specific activity of the purified Ca^{2+}-ATPase from plasma membranes independent of enzyme concentration. *Biochim. Biophys. Acta.* 1420: 57–62.

Castello, P. R., A. J. Caride, F. L. González Flecha, H. N. Fernandez, J. P. Rossi, and J. M. Delfino. 1994. Identification of transmembrane domains of the red cell calcium pump with a new photoactivatable phospholipidic probe. *Biochem. Biophys. Res. Commun.* 201:194–200.

Cavieres, J. D. 1984. Calmodulin and the target size of the ($Ca^{2+}+Mg^{2+}$)-ATPase of human red-cell ghosts. *Biochim. Biophys. Acta.* 771:241–244.

Chen, P. S., T. Y. Toribara, and H. Warner. 1956. Microdetermination of phosphorus. *Anal. Chem.* 28:1756–1758.

Coelho-Sampaio, T., S. T. Ferreira, G. Benaim, and A. Vieyra. 1991. Dissociation of purified erythrocyte Ca^{2+}-ATPase by hydrostatic pressure. *J. Biol. Chem.* 266:22266–22272.

de Levie, R. 1999. Estimating parameter precision in nonlinear least squares with Excel's Solver. *J. Chem. Ed.* 76:1594–1598.

Donnet, C., A. J. Caride, S. Talgham, and J. P. Rossi. 1998. Chemical modification reveals involvement of different sites for nucleotide analogues in the phosphatase activity of the red cell calcium pump. *J. Membr. Biol.* 163:217–224.

Filoteo, A. G., J. P. Gorski, and J. T. Penniston. 1987. The ATP-binding site of the erythrocyte membrane Ca^{2+} pump. Amino acid sequence of the fluorescein isothiocyanate-reactive region. *J. Biol. Chem.* 262: 6526–6530.

Fiske, C. H., and Y. Subbarow. 1925. The colorimetric determination of phosphorous. *J. Biol. Chem.* 66:375–400.

Garrahan, P., and A. F. Rega. 1990. Plasma membrane calcium pump. *In* Intracellular Calcium Regulation. F. Bronner, editor. Wiley-Liss, New York. 271–303.

Gatto, C., and M. A. Milanick. 1993. Inhibition of the red blood cell calcium pump by eosin and other fluorescein analogues. *Am. J. Physiol. Cell Physiol.* 264:C1577–C1586.

González Flecha, F. L., P. R. Castello, A. J. Caride, J. J. Gagliardino, and J. P. Rossi. 1993. The erythrocyte calcium pump is inhibited by non-enzymic glycation: studies in situ and with the purified enzyme. *Biochem. J.* 293:369–375.

Kosk-Kosicka, D., and T. Bzdega. 1988. Activation of the erythrocyte Ca^{2+}-ATPase by either self-association or interaction with calmodulin. *J. Biol. Chem.* 263:18184–18189.

Kosk-Kosicka, D., and T. Bzdega. 1990. Effects of calmodulin on erythrocyte Ca^{2+}-ATPase activation and oligomerization. *Biochemistry.* 29: 3772–3777.

Kosk-Kosicka, D., T. Bzdega, and A. Wawrzynow. 1989. Fluorescence energy transfer studies of purified erythrocyte Ca^{2+}-ATPase. Ca^{2+}-regulated activation by oligomerization. *J. Biol. Chem.* 264: 19495–19499.

Kosk-Kosicka, D., M. M. Lopez, I. Fomitcheva, and V. L. Lew. 1995. Self-association of plasma membrane Ca^{2+}-ATPase by volume exclusion. *FEBS Lett.* 371:57–60.

Lakowicz, J. 1983. Principles of Fluorescence Spectroscopy. Plenum Press, New York.

Levi, V., J. P. Rossi, P. R. Castello, and F. L. Gonzalez-Flecha. 2000a. Oligomerization of the plasma membrane calcium pump involves two regions with different thermal stability. *FEBS Lett.* 483:99–103.

Levi, V., J. P. Rossi, M. M. Echarte, P. R. Castello, and F. L. González Flecha. 2000b. Thermal stability of the plasma membrane calcium pump. Quantitative analysis of its dependence on lipid–protein interactions. *J. Membr. Biol.* 173:215–225.

Minocherhomjee, A., G. Beauregard, M. Potier, and B. Roufogalis. 1983. The molecular weight of the calcium-transport-ATPase of the human red blood cell determined by radiation inactivation. *Biochem. Biophys. Res. Commun.* 116:895–900.

Møller, J. V., B. Juul, and M. le Maire. 1996. Structural organization, ion transport, and energy transduction of P-type ATPases. *Biochim. Biophys. Acta.* 1286:1–51.

Munkonge, F., E. K. Michelangely, E. K. Rooney, J. M. East, and A. G. Lee. 1988. Effect of phospholipid:protein ratio on the state of aggregation of the (Ca^{2+}-Mg^{2+})-ATPase. *Biochemistry.* 27:6800–6805.

Papp, S., S. Pikula, and A. Martinosi. 1987. Fluorescence energy transfer as an indicator of Ca^{2+}-ATPase interactions in sarcoplasmic reticulum. *Biophys. J.* 51:205–220.

Pikula, S., A. Wrzosek, and K. S. Famulski. 1991. Long-term stabilization and crystallization of ($Ca^{2+}+Mg^{2+}$)-ATPase of detergent-solubilized erythrocyte plasma membrane. *Biochim. Biophys. Acta.* 1061:206–214.

Sackett, D. L., and D. Kosk-Kosicka. 1996. The active species of plasma membrane Ca^{2+}-ATPase are a dimer and a monomer-calmodulin complex. *J. Biol. Chem.* 271:9987–9991.

Schmid, F. X. 1992. Kinetics of unfolding and refolding of single-domain proteins. *In* Protein Folding. T. E. Creighton, editor. W. H. Freeman and Company, New York. 197–241.

Seber, G. A. F., and C. J. Wild. 1989. Nonlinear Regression. John Wiley and Sons, New York.

Silva, J. L., E. W. Miles, and G. Weber. 1986. Pressure dissociation and conformational drift of the beta dimer of tryptophan synthase. *Biochemistry.* 25:5780–5786.

Toyoshima, C., M. Nakasako, H. Nomura, and H. Ogawa. 2000. Crystal structure of the calcium pump of sarcoplasmic reticulum at 2.6 Å resolution. *Nature.* 405:599–718.

Veatch, W. and L. Stryer. 1977. The dimeric nature of the gramicidin A transmembrane channel: conductance and fluorescence energy transfer studies of hybrid channels. *J. Mol. Biol.* 113:89–102.

Vilsen, B., J. P. Andersen, J. Petersen, and P. L. Jørgensen. 1987. Occlusion of $^{22}Na^+$ and $^{86}Rb^+$ in membrane-bound and soluble protomeric alpha beta-units of Na, K-ATPase. *J. Biol. Chem.* 262:10511–10517.

Weber, G. 1987. Dissociation of oligomeric proteins by hydrostatic pressure. *In* High Pressure Chemistry and Biochemistry. R. Van Eldik and J. Jonas, editors. D. Reidel Publishing Company, Dordrecht, The Netherlands. 401–420.